

Emission spectra of KrXeCl, KrXeBr, KrXeI, ArKrF, and ArKrCl

H. C. Brashears, D. W. Setser, and Y.C. Yu

Citation: *J. Chem. Phys.* **74**, 10 (1981); doi: 10.1063/1.440863

View online: <http://dx.doi.org/10.1063/1.440863>

View Table of Contents: <http://jcp.aip.org/resource/1/JCPSA6/v74/i1>

Published by the [American Institute of Physics](#).

Additional information on *J. Chem. Phys.*

Journal Homepage: <http://jcp.aip.org/>

Journal Information: http://jcp.aip.org/about/about_the_journal

Top downloads: http://jcp.aip.org/features/most_downloaded

Information for Authors: <http://jcp.aip.org/authors>

ADVERTISEMENT



www.goodfellowusa.com

Goodfellow

metals • ceramics • polymers • composites

70,000 products

450 different materials

small quantities *fast*

Emission spectra of KrXeCl^* , KrXeBr^* , KrXeI^* , ArKrF^* , and ArKrCl^*

H. C. Brashears, Jr., D. W. Setser, and Y.-C. Yu

Chemistry Department, Kansas State University, Manhattan, Kansas 66506
(Received 16 June 1980; accepted 23 September 1980)

Sensitized reactions of Xe and Kr with halogen donors in the presence of high buffer gas pressures of Kr and Ar, respectively, have led to the observation of five emission bands in the ultraviolet region of the spectrum. These broad structureless bands are assigned to the mixed rare gas-halide trimers KrXeCl^* , KrXeBr^* , KrXeI^* , ArKrF^* , and ArKrCl^* . Despite an extensive search, no emission corresponding to KrXeF^* could be found and this mixed trimer may be unstable because of interaction with a lower repulsive state. The positions and half-widths of the five emission bands are characterized, and the formation mechanism of the mixed trimers in these experiments is discussed.

INTRODUCTION

The homonuclear rare gas halide triatomic molecules Ar_2F^* , Ar_2Cl^* , Kr_2F^* , Kr_2Cl^* , and Xe_2Cl^* have been observed in emission,¹⁻⁴ and calculations^{5,6} of the relevant potentials are available for Ar_2F^* and Kr_2F^* . Only one upper state is expected to be bound relative to dissociation to $\text{RgX}^* + \text{Rg}$. The upper state is ionic (Rg_2^+X^-) in nature and the lower states, which are all repulsive, are covalent states. We have observed emission bands from five heteronuclear rare gas halide triatomic molecules KrXeCl^* , KrXeBr^* , KrXeI^* , ArKrF^* , and ArKrCl^* during our study⁷ of the $\text{Xe}(^3P_1)$ and $\text{Kr}(^3P_1)$ resonance state reactions with halogen donors at high pressure of Kr or Ar, respectively, as buffer gases, i. e., Kr with $\text{Xe}(^3P_1)$ and Ar with $\text{Kr}(^3P_1)$. Attempts were made to observe KrXeF^* , but no emission could be found corresponding to this molecule even under conditions which yielded the other KrXeX^* molecular emissions. The new emissions are broad structureless bands lying slightly to longer wavelength of the $\text{RgX}(C-A)$ emission band; their intensities increase, relative to the KrX^* or XeX^* emission, with increasing pressure of the buffer gas and they become the dominant emission at sufficiently high pressures.

A previous claim⁸ in the literature for KrXeF^* and ArKrF^* emission bands is inconsistent with our observations. The mixed rare gas halide trimers have been postulated³ from the magnitudes of some of the three-body rare gas halide quenching rate constants and our observations support those suggestions for Ar with KrF^* and KrCl^* , for Kr with XeCl^* , XeBr^* , and XeI^* , but not Kr with XeF^* .

In previous work⁷ we have reported on the low pressure XeX^* and KrX^* ($\text{X} = \text{Cl}, \text{F}$) emission spectra from the reactions of $\text{Xe}(^3P_1)$ and $\text{Kr}(^3P_1)$ with chlorine and fluorine donors. We demonstrated that the $(^3P_1)$ resonance states reacted in the same way as the metastable $(^3P_2)$ states of Kr and Xe with regard to branching fraction for rare gas halide formation and for vibrational energy disposal to XeX^* and KrX^* . With the sensitization technique lighter rare gases can be added to the cell and the rare gas halide emission can be studied at high pressures of these buffer gases. Such experiments⁷ confirmed that $\text{XeF}(C)$ was lower in energy than $\text{XeF}(B)$ and suggested the same ordering for XeCl^* , KrF^* , and

possibly KrCl^* . In this paper we report the mixed rare gas halide trimer spectra and some qualitative features related to the XeX^* and KrX^* relaxation. The state-to-state relaxation of XeCl^* in He, Ne, Ar, Kr, and N_2 buffer gases will be reported separately.⁹

EXPERIMENTAL

The experimental technique⁷ is the same as used by others^{10,11} for observing reactions of the rare gas resonance states. The cell used for this study is unchanged from our previous work.^{7,12} A microwave powered discharge lamp was interfaced to a stainless-steel reaction vessel via a MgF_2 (or sapphire) window; the emission spectra were observed through a quartz window at right angles to the light from the resonance lamp. The homemade lamp was attached to the cell via an O-ring seal. When the Xe and Kr lamps were operating, the 5-7 cm extension arm was cooled with liquid Ar or liquid N_2 , respectively. The emission spectra from the lamps, examined with a vacuum monochromator, consisted predominantly of the $(^3P_1)$ resonance lines (147.0 nm for Xe, 123.6 nm for Kr). There also is strong atomic emission in the visible and red regions, but these do not interfere with the present measurements.

Static mixtures could be used for F_2 and Cl_2 donor molecules. We selected CBr_4 and CF_3I as bromine and iodine donors rather than Br_2 or I_2 , because of gas handling ease in the stainless vessel. Bromine and iodine also give some interfering molecular emission from the $(^3P_1)$ atom reactions, which causes some complication. Premixed CF_3I (or CBr_4) and Xe mixtures were slowly flowed through the cell to obtain good low pressure XeI^* and XeBr^* spectra. Flowing was necessary; otherwise the emission intensity slowly varied in time and other (Br_2^* or I_2^*) emission developed from accumulation of products in the cell. For high pressure experiments flowing the gases was not feasible and static experiments with frequent refilling of the cell was employed. The partial pressures of the components in the cell were measured with a pressure transducer. The Xe or Kr pressure is typically 0.02 Torr, the reagent pressure is 0.05 Torr, and the Kr or Ar buffer gas varied from a few to 3000 Torr. Possible rupture of the windows restricted the total pressure to less than 5 atm.

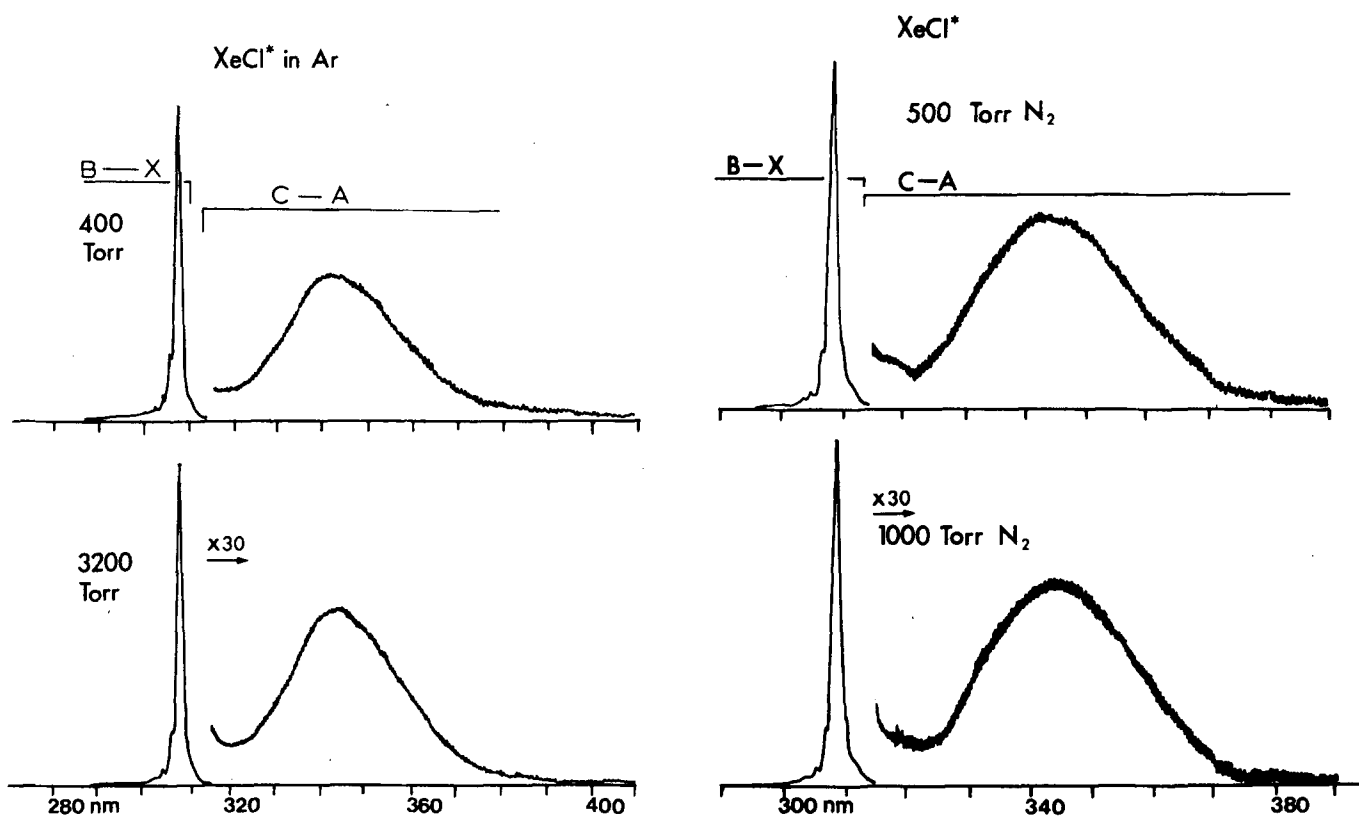


FIG. 1. Sensitized XeCl^* emission spectra from Xe/Cl_2 mixture and various pressures of Ar or N_2 bath gas; $\text{Xe} \sim 10$ mTorr and $\text{Cl}_2 \approx 50$ mTorr. Spectra are corrected for monochromator response. (a) XeCl^* emission spectra in 400 and 3200 Torr of Ar. (b) XeCl^* emission spectra in 500 and 1000 Torr of N_2 .

The emission was viewed with a 0.75 m Jarrell Ash monochromator fitted with an EMI 9558Q photomultiplier tube. The photomultiplier tube signal is recorded by a photon counter. Both the monochromator and photon

counter are interfaced to a PDP-8 computer. The spectra are stored on tape and subsequently corrected for wavelength response of the detection system. Integration of the emission intensities, subtraction of back-

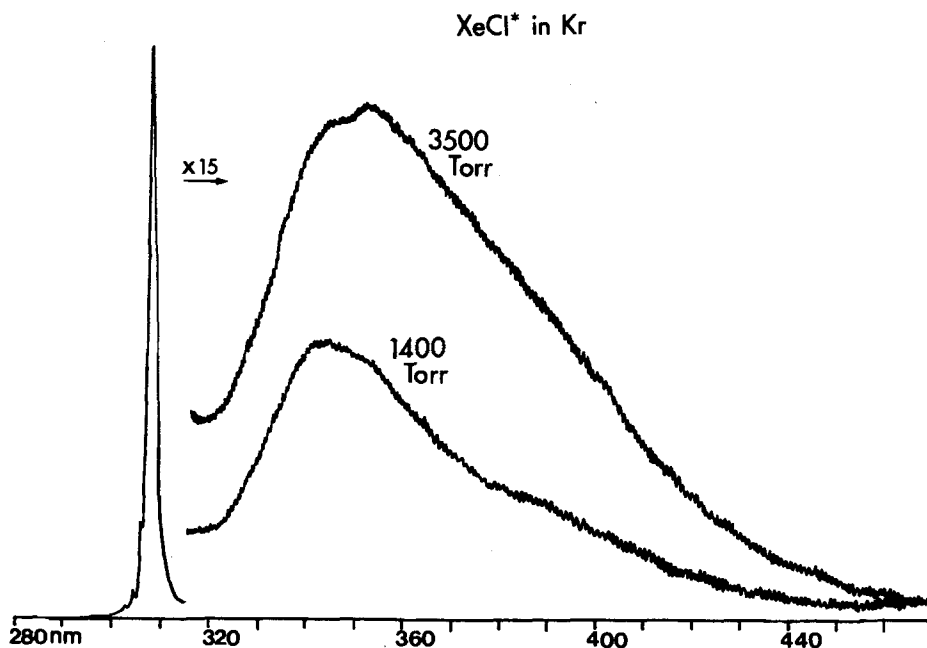


FIG. 2. Observed XeCl^* and KrXeCl^* emission spectra from sensitization of Xe/Cl_2 mixture ($\text{Xe} \sim 10$ mTorr and $\text{Cl}_2 \approx 50$ mTorr) with 1400 and 3500 Torr of Kr. Spectra are corrected for monochromator response.

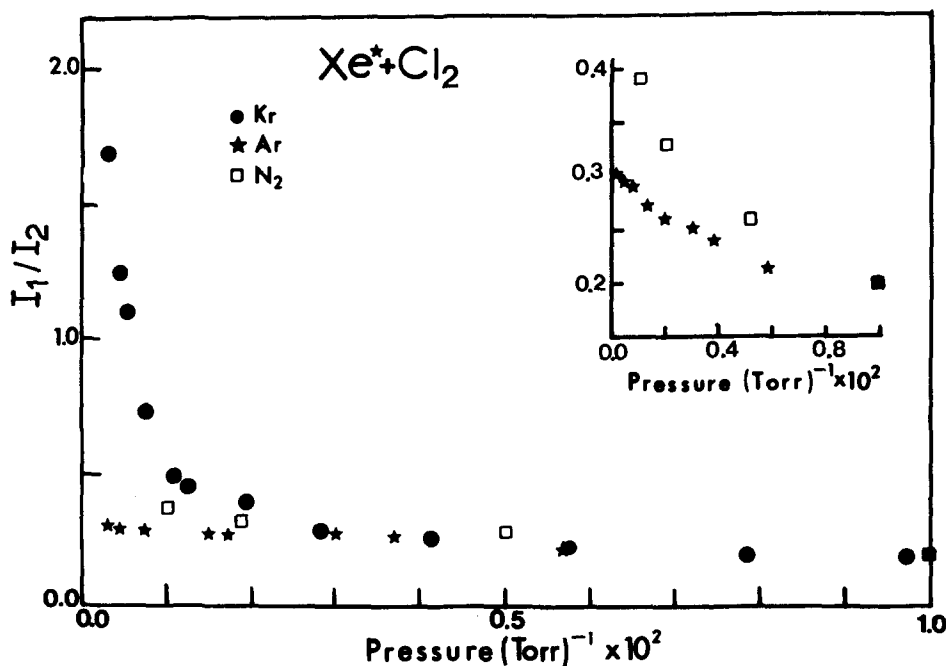


FIG. 3. Ratio I_1/I_2 of integrated emission intensities for sensitization of Xe/Cl₂ mixture in Ar, N₂, and Kr buffer gas. I_2 integrated intensity from 316–280 nm; I_1 integrated intensity from 316–460 nm. For Ar and N₂ bath gas this ratio corresponds to $I_{\text{XeCl}(C-A)}/I_{\text{XeCl}(B-X)}$ if the small contribution to I_1 from the XeCl(B-A) transition is ignored.

ground, etc. is done with the computer. All spectra shown in this paper are computer generated and corrected for wavelength response of the detection system.

RESULTS

We first show (Fig. 1) some characteristic spectra of XeCl* at various pressures of Ar and N₂ from sensitization of Xe/Cl₂ mixtures. These spectra identify the bandwidth of the XeCl(C-A) transition at pressures sufficiently high that the XeCl(B) and XeCl(C) vibrational distributions are 300 K Boltzmann. The contribution of the XeCl(B-A) transition to the 345 nm band is estimated as ~ 15% based upon the relative intensity of the B-X band and the theoretical B-A/B-X transition ratio. The B-A contribution to the C-A band is not of importance to this work and we will not consider the XeCl(B-A)

transition further. Figure 2 shows characteristic spectra in the Xe/Cl₂ sensitized system with ≥ 1000 Torr of Kr bath gas. There is a systematic growth of a new band, with a maximum at ~ 370 nm, with increasing Kr pressure. This increase in intensity to the longer wavelength side of the XeCl(C-A) band is shown by the very large increase in the ratio (I_1/I_2) of integrated intensities for Kr buffer relative to this ratio in Ar or N₂ (see Fig. 3). The I_1 intensity is the sum of the XeCl(C-A) and KrXeCl* emissions, and I_2 is the XeCl(B-X) emission intensity. The KrXeCl* band was deconvoluted from the XeCl(C-A) emission by a point by point subtraction of the XeCl(C-A) emission from the combined emission, after normalization of both spectra to the same XeCl(B-X) peak height and correction for monochromator response (see Fig. 4). For example, the

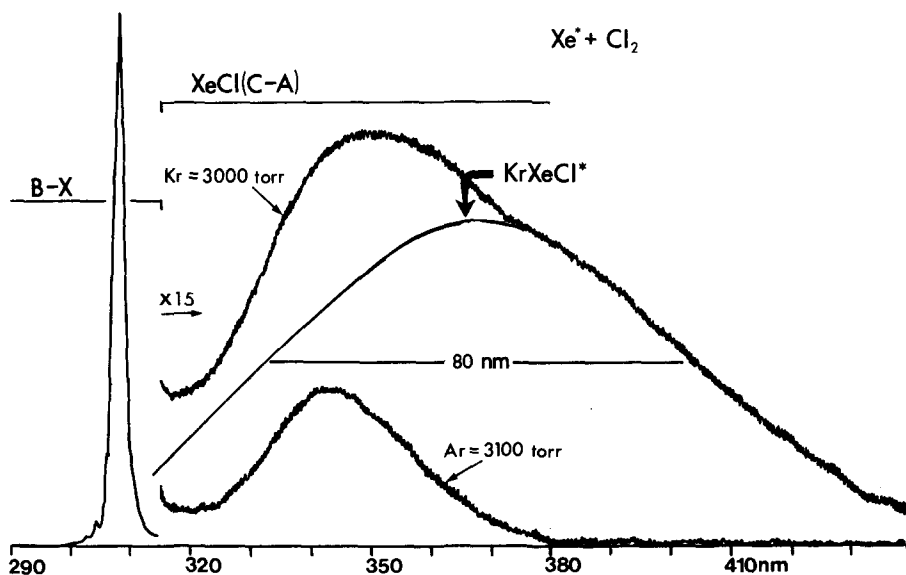


FIG. 4. Comparison of the observed emission spectra from sensitized Xe/Cl₂ mixture (Xe ~ 10 mTorr and Cl₂ ~ 50 mTorr) in 3000 Torr of Ar and Kr. The band assigned to KrXeCl* is obtained by deconvolution; see the text. Spectra are corrected for monochromator response.

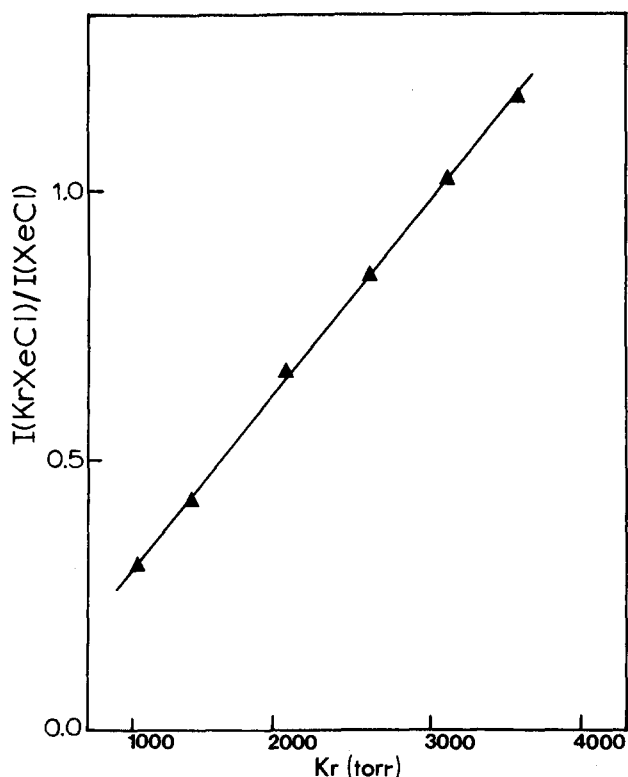


FIG. 5. The KrXeCl*/XeCl* emission intensity ratio as a function of Kr pressure.

XeCl(B-X) band in Kr was normalized to the same height observed for XeCl(B-X) in Ar(3500 Torr); then the XeCl(C-A) band in Ar was subtracted from the observed spectrum in Kr. To insure that some unknown emission was not causing an error, the deconvolution pro-

cedure was repeated using the XeCl* spectrum obtained in N₂(500 Torr) in place of the spectrum in Ar (3500 Torr); the same KrXeCl* band was obtained.

Absolute emission intensities can not be reliably measured in our experiments, so the emission intensity of KrXeCl* was compared to that of XeCl(B and C). The KrXeCl*/XeCl* emission intensity ratio is plotted vs Kr pressure in Fig. 5. This plot reveals two points: (1) At pressures > 3000 Torr the KrXeCl* emission intensity is stronger than the XeCl* emission intensity, and (2) the KrXeCl*/XeCl* intensity ratio is linear in Kr pressure from 1000 to 3500 Torr.

An additional point of interest is the XeCl(B)/XeCl(C) ratio for various pressures of Ar, N₂, and Kr; those data are shown in Fig. 3. The Ar data (plotted formerly as a concentration ratio) are the same as shown in Ref. 6. Both Kr and N₂ cause rapid XeCl* vibrational relaxation and B/C state mixing. Although the XeCl* emission becomes rather weak because of quenching of Xe(³P₁) by N₂, the high pressure I_C/I_B intercept is $\lesssim 0.3$ and close to that found for Ar buffer gas. Thus, the N₂ data corroborate the state ordering reported in Ref. 7, i. e., the XeCl(C) state is below the XeCl(B) state. With Kr the C/B ratio goes through the minimum at ~ 100 Torr and then begins rising at higher pressure (see Fig. 3) before the KrXeCl emission is observed. Extrapolation of the Kr points, which do not show any KrXeCl* emission, to infinite pressure also suggests an equilibrium I_C/I_B ratio of ~ 0.3 . Based upon the temperature variation of the XeCl(B-X) and Xe(C-A) intensity ratio, Tellinghuisen also has concluded in favor of the XeCl(C) state being slightly below the XeCl(B) state.¹³

After characterization of the KrXeCl* emission, ex-

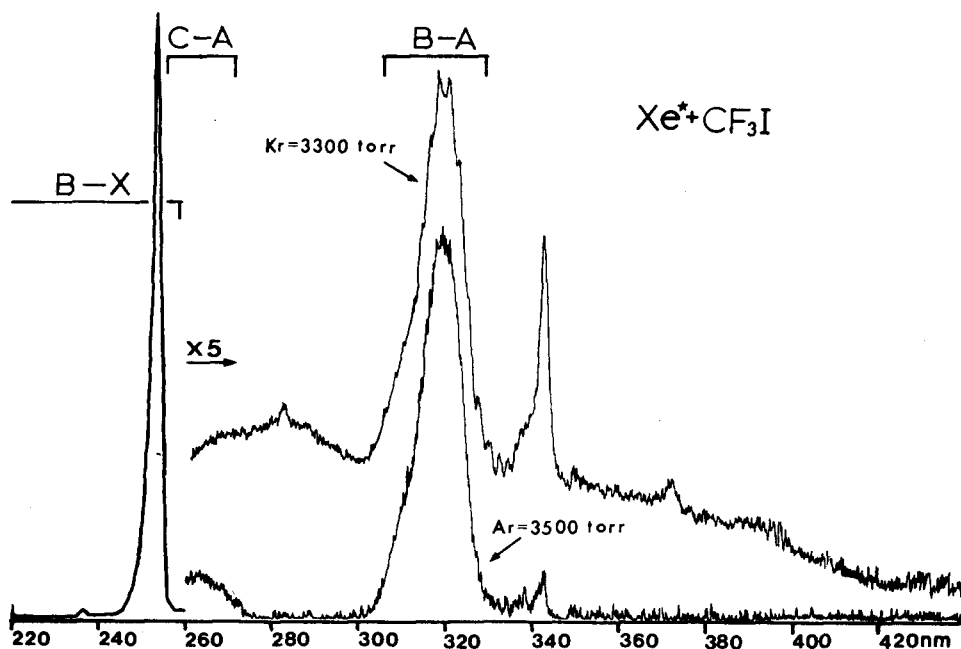


FIG. 6. Comparison of the emission observed from sensitized Xe/CF₃I mixture (Xe \approx 30 mTorr, CF₃I \approx 100 mTorr) in 3500 Torr of Ar and Kr. The three XeI bands, which are fully resolved in the Ar spectrum, are labeled. The sharp band at ~ 342 nm is I₂ emission from I₂ contamination. In each spectrum the XeI(B-X) band is normalized to the same height.

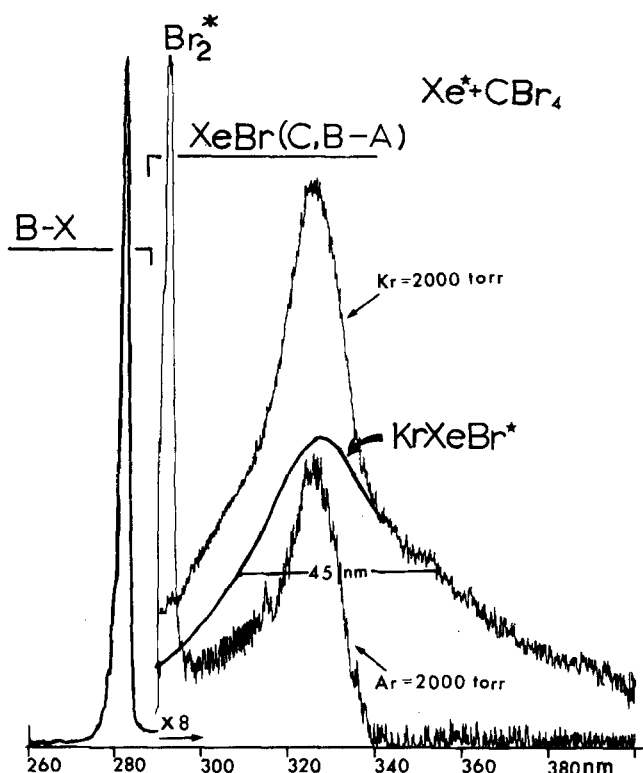


FIG. 7. The KrXeBr^* emission spectra from deconvolution of the emission observed in 2000 Torr of Kr and Ar from sensitization of a Xe/CBr_4 mixture ($\text{Xe} \approx 30$ mTorr and $\text{CBr}_4 \approx 100$ mTorr). Spectra are corrected for monochromator response. The $\text{XeBr}(B-A)$ and $\text{XeBr}(C-A)$ bands are overlapped. In each spectrum the $\text{XeBr}(B-X)$ bands are normalized to the same height. The sharp band at 292 nm in the spectrum with 2000 Torr of Ar is a Br_2 emission that is thought to arise from reaction of Br_2 that accumulates from sensitization and/or photolysis of CBr_4 .

periments were done with Xe/F_2 , Xe/CBr_4 , and $\text{Xe}/\text{CF}_3\text{I}$ mixtures in Kr and Ar bath gases and searches were made for the KrXeF^* , KrXeBr^* , and KrXeI^* emission bands. The results for KrXeBr^* and KrXeI^* are shown in Figs. 6 and 7. For these cases accurate deconvolution of the $\text{XeBr}(C, B-A)$ and $\text{XeI}(C, B-A)$ bands from the trimer emissions is more difficult than for the XeCl^* and KrXeCl^* pair. However, comparison of the high pressure spectra obtained in Kr to that obtained in Ar definitely identify a broad band emission that we assign to KrXeI^* and KrXeBr^* . The KrXeBr^* position and half-width can be assigned with reasonable certainty; however, the KrXeI^* emission tails to long wavelength and appears to extend from 260 to 420 nm. This breadth may be associated with the large splitting of the lower KrXeI states from the spin-orbit energy difference of $I(^2P_{1/2})$ and $I(^2P_{3/2})$.

An extensive search from 350–700 nm was made for KrXeF^* using sensitization of Xe/F_2 mixtures with added Kr pressures up to 3000 Torr; no evidence could be found for a new emission system to the red of the $\text{XeF}(C-A)$ band. This is a difficult region for us to observe because of scattered atomic Xe lines from the discharge. Nevertheless, we should have been able to

observe a band if it was present. We did observe relaxation of $\text{XeF}(B)$ and $\text{XeF}(C)$ with development of the characteristic broad band, which peaks at ~ 470 nm, of the vibrationally relaxed $\text{XeF}(C-A)$ transition.¹² Two unusual features, relative to the other $\text{XeX} + \text{Kr}$ systems, were found: (i) At low Kr pressure the endoergic displacement¹⁴ of Xe from highly vibrationally excited XeF^* with formation of $\text{KrF}(B)$ seemed to occur. (ii) At pressures above 400 Torr of Kr, a strong reduction in XeF^* emission intensity was noted: This XeF^* quenching was much stronger than would be expected based upon the measured quenching rate constant of XeF^* generated by the photolysis¹² of XeF_2 . This strong XeF^* quenching was not observed in Ar buffer.

Emission bands corresponding to ArKrF^* and ArKrCl^* were obtained from sensitization experiments with Kr/F_2 and Kr/Cl_2 mixtures in Ar buffer. These broad emissions, which appear to the red of the $\text{KrF}(C-A)$ and $\text{KrCl}(C-A)$ bands, are shown in Figs. 8 and 9. The ArKrCl^* band is resolved from the $\text{KrCl}(C-A)$ band and no deconvolution is necessary. The sharp Cl_2 emission band generated by the $\text{Kr}(^3P_1) + \text{Cl}_2$ reaction that is superimposed upon the ArKrCl^* emission can be subtracted by hand to get the ArKrCl^* emission band. Deconvolution is required to separate the ArKrF^* and $\text{KrF}(C-A)$ emission bands. This deconvolution was done using the KrF^* spectra obtained with Ne buffer as the reference in the way previously described for the KrXeCl^* and $\text{XeCl}(C-A)$ bands.

DISCUSSION

The positions and half-widths of the $\text{Rg}'\text{RgX}^*$ emissions observed in this report are summarized in Table I. Results for the Rg_2X^* emissions also are included for comparison. The mixed rare gas trimer bands occur at shorter wavelength than the Rg_2X trimer bands by the following amounts: $\text{ArKrF}^* - 95$ nm, $\text{ArKrCl}^* - 55$ nm, and $\text{KrXeCl}^* - 120$ nm. This is to be expected because the upper states arising from $\text{Rg}'\text{Rg}^*$ are more weakly bound than the Rg_2^* states, whereas the repulsive lower states are not so different. Our assignment (335 nm) for the ArKrF^* band differs greatly from that (420 nm) of Basov *et al.*⁸ Their assignment would place ArKrF^* 20 nm to the red of the currently well established Kr_2F^* band, which is quite unrealistic. The 480 nm band that Basov *et al.* assigned to KrXeF^* most likely is the $\text{XeF}(C-A)$ emission which peaks at ~ 470 nm. We believe our assignments in Table I to be correct.

As illustrated by the location of the observed $\text{Rg}'\text{RgX}^*$ bands, the KrXeF^* band is expected to be to the red side of the $\text{XeF}(C-A)$ transition. Before discussing the lack of emission from KrXeF^* (and Xe_2F^*), the $\text{Rg}'\text{RgX}$ formation mechanism will be considered.

The following steps were considered for $\text{Xe}(^3P_1)$ sensitization in a Kr/Cl_2 mixture:



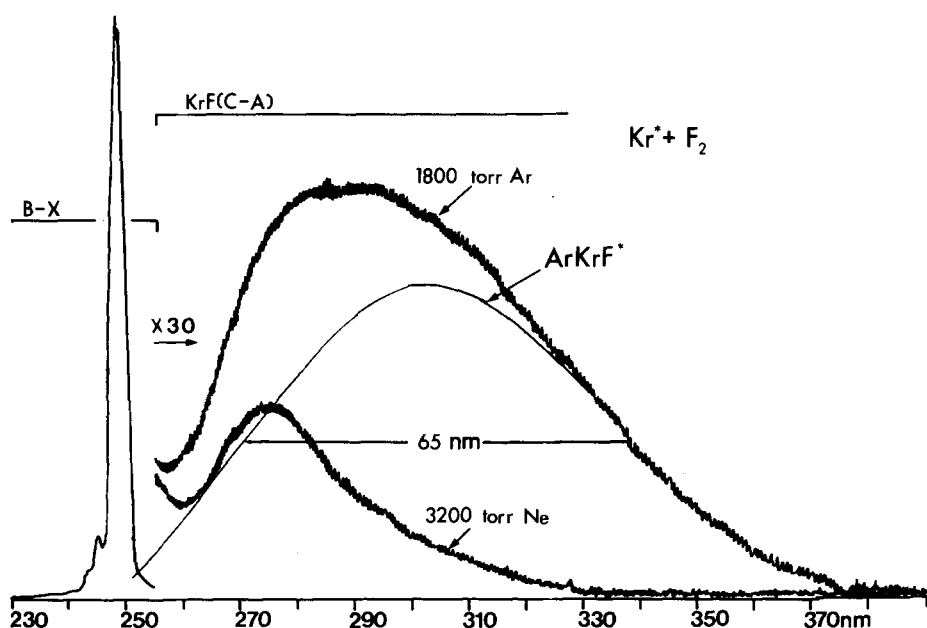


FIG. 8. The ArKrF* emission spectra from deconvolution of the emission observed from a sensitized Kr/F₂ mixture (Kr ~ 20 mTorr and F₂ ≈ 50 mTorr) is 1800 Torr of Ar and 3200 Torr of Ne. Spectra are corrected for monochromator response. In each spectrum the KrF(B-X) band is normalized to the same height.

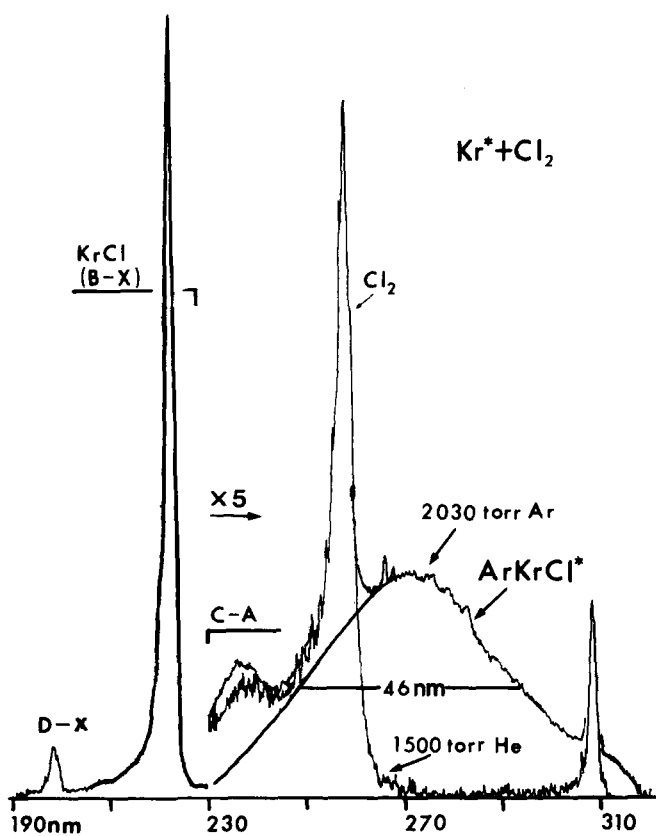
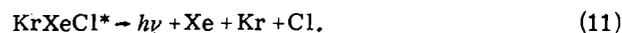
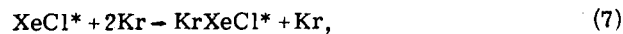
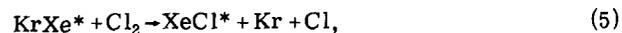


FIG. 9. The ArKrCl* emission deconvoluted from sensitization of Kr/Cl₂ mixtures (Kr ≈ 20 mTorr and Cl₂ ≈ 50 mTorr) from 2030 Torr Ar and 1500 Torr He. Note the relatively well resolved KrCl(C-A) and ArKrCl emission bands. The sharp band at ~258 nm is the Cl₂ emission excited by the Kr(³P₁) + Cl₂ reaction. In each spectrum the KrCl(B-X) band is normalized to the same height.



In the absence of Kr there is only the competition between radiative decay of Xe(³P₁) and reaction with Cl₂,

TABLE I. Summary of rare gas halide trimer emission bands.

RgRg'X	Position (nm)	Half-width (nm)	Reference ^a
Ar ₂ F	292	53	1, 2
Ar ₂ Cl	246	...	1
Kr ₂ F	400	60	1, 8
Kr ₂ Cl	325	33	1
Xe ₂ Cl	490	80	3
ArKrF	305	65	This work
ArKrCl	270	46	This work
KrXeCl	370	80	This work
KrXeBr	330	45	This work
KrXeI	~290	Unsymmetrical, tails to red	This work

^aThe Rg₂X emission bands have been observed by several laboratories and the list given here is only to characterize their locations and half-widths.

with a rate constant¹⁵ of $\sim 7 \times 10^{-10} \text{ cm}^3 \text{ molecule}^{-1} \text{ s}^{-1}$. As Kr is added there is two-body transfer to $\text{Xe}(^3P_2)$, which we will ignore, and three-body KrXe^* formation with an assumed rate constant of $\sim 1 \times 10^{-32} \text{ cm}^6 \text{ s}^{-1}$ [the rate constant for $\text{Kr}(^3P_2) + 2\text{Ar}$ is $1.2 \times 10^{-32} \text{ cm}^6 \text{ s}^{-1}$].¹⁶ At 500 Torr of Kr and 50 mTorr of Cl_2 the rate of loss of Xe^* by Reaction (1) is $1 \times 10^6 \text{ s}^{-1}$ and that by Reaction (3) is $2 \times 10^6 \text{ s}^{-1}$. Thus, above 500 Torr of Kr we can expect the KrXe^* molecule to be important in the kinetic scheme. Since the rate constant for quenching KrXe^* by Cl_2 will be as large for Xe^* ,¹⁷ the main limitation to the importance of KrXe^* in the subsequent kinetics will be its radiative lifetime. The lifetime is not so simple to evaluate since three-body combination presumably produces both $\text{KrXe}^*(^3\Sigma^+)$ and $\text{KrXe}^*(^1\Sigma^+)$. The lifetime of KrXe^* has not been studied; but the values for $\text{Xe}_2(1_u)$ and $\text{Xe}_2(0_u^+)$ are ~ 100 and ~ 5 ns, respectively.^{18,19} Since the Cl_2 pressure is ≈ 0.05 Torr, the expected short lifetime of $\text{KrXe}^*(^1\Sigma^+)$ implies that only $\text{KrXe}^*(^3\Sigma^+)$ could be involved in step (4). Qualitatively, we observed only modest (factor of 5–10) loss in the XeCl^* , XeBr^* , or XeI^* signal intensity with added Kr (or Ar), implying that the KrXe^* lifetime must be > 200 ns. (The quenching, however, is much different for addition of Kr to the Xe/F_2 system as will be discussed below). The KrXe^* lifetimes are expected to be somewhat longer than for Xe_2^* , because of the weaker bonding for the former.

The reaction dynamics for $\text{KrXe}^* + \text{Cl}_2$ should involve the $\text{KrXe}^*, \text{Cl}_2$ potential just as the $\text{Xe}(^3P_{2,1}) + \text{Cl}_2$ reactions involve the Xe^*, Cl_2 potential. The latter gives a large fraction of highly vibrationally excited XeCl^* molecules.²⁰ Therefore, we expect the initially formed KrXeCl^* molecules to be vibrationally excited; these molecules will dissociate to XeCl^* , since $D(\text{Kr}-\text{XeCl}^*)$ is $\lesssim 0.3$ eV.²¹ This conclusion about $\text{RgRg}^* + \text{X}_2$ reactions also has been advocated by others.^{6,22} Thus, it does not matter whether Reaction (5) or (6) is the primary exit channel from quenching KrXe^* by Cl_2 because formation of XeCl^* will be the end result. Providing that $\tau(\text{KrXe}^*)$ is sufficiently long that quenching of KrXe^* by Cl_2 dominates over radiative decay, step (3) is of little importance in the kinetic scheme since each Xe^* is still converted to one XeCl^* molecule.

Since $\text{KrXe}^* + \text{Cl}_2$ does not directly give KrXeCl^* , the KrXeCl^* formation mechanism is likely to be three-body recombination of XeCl^* with 2Kr [Reaction (7)]. If this is the case, then the steady-state ratio of KrXeCl^* to XeCl^* emission intensities is given by

$$\frac{I_{\text{KrXeCl}^*}}{I_{\text{XeCl}^*}} = \frac{\tau_{\text{KrXeCl}^*}^{-1} k_7 [\text{XeCl}^*] [\text{Kr}]^2}{\tau_{\text{XeCl}^*}^{-1} [\text{XeCl}^*]} \cdot \frac{1}{\tau_{\text{KrXeCl}^*}^{-1} + k_{10} [\text{Kr}]} \quad (12)$$

This expression is consistent with the linear plot shown in Fig. 5 providing that $k_{10}[\text{Kr}] > \tau_{\text{KrXeCl}^*}^{-1}$. Quigley and Hughes²² have reported a $\tau(\text{Kr}_2\text{F}^*)$ of 181 ns and an upper limit to the quenching of Kr_2F^* by Kr of $2 \times 10^{-14} \text{ cm}^3 \text{ s}^{-1}$. If these values are adopted for KrXeCl^* in Kr, radiative decay of KrXeCl^* would dominate our collisional quenching and Fig. 5 would be second order in Kr pres-

sure. Based upon this preliminary analysis, a value of k_{10} near $10^{-13} \text{ cm}^3 \text{ s}^{-1}$ [assuming $\tau(\text{XeKrCl}^*) \approx 200$ ns] is favored.

In terms of the above mechanism, the failure to observe any ArXe^* trimer emission is explained by Reaction (7) being slow with Ar as the third body. This is expected since $(\text{ArXe})^*$ is bound by only $0.14 (\pm 0.02)$ eV, whereas $(\text{KrXe})^*$ is bound by $0.37 (\pm 0.02)$ eV.²¹ Therefore, the binding in $(\text{ArXe})^*\text{X}^-$ is expected to be vanishingly small. A similar argument applies to the NeKrX^* trimers. However, the ArKrBr^* trimer is expected to be a stable molecule. Since KrI^* is largely, but not totally, predissociated²³ to $\text{I}^* + \text{Kr}$, the ArKrI^* trimer may be unstable; on the other hand, the ~ 0.3 eV binding of ArKr^*I^- relative to $\text{KrI}^* + \text{Ar}$ could lower the bound state potential to below the surface crossing to $\text{I}^* + \text{Kr} + \text{Ar}$. A definitive answer to the existence of ArKrI^* awaits experimental test. Further experiments with observation at shorter wavelength is required to identify ArKrBr^* and ArKrI^* .

The failure to observe emission from a KrXeF^* trimer from sensitized experiments of Xe/F_2 mixtures in Kr bath gas is in striking contrast to the other KrXeX^* cases. However, the sensitized observations are supported by the absence of detectable KrXeF^* emission in the 400–700 nm region from photolysis experiments of XeF_2 in 3000 Torr of Kr bath gas.¹² In these experiments the scattered light from the photolysis lamp is not severe and the detection limit is much higher than in the sensitization experiments. A parallel seems to exist with Xe_2F^* , which also has not been observed despite our efforts (photolysis of XeF_2 in the presence of 3000 Torr of Xe and searches for emission from 400 to 800 nm)¹² as well as others, to find such an emission. There is a strong possibility that the ionic bound states of both Xe_2F^* and KrXeF^* are unstable with respect to a potential surface crossing with the highest member of the repulsive covalent curves.⁶ This assumption can explain the absence of KrXeF^* or Xe_2F^* emission. However, we still need to explain the rather strong overall quenching of XeF^* in sensitization of Xe/F_2 mixtures upon addition of ≥ 400 Torr of Kr. Furthermore, the explanation must be consistent with the rather slow ($k = 1.0 \pm 0.3 \times 10^{-13} \text{ cm}^3 \text{ s}^{-1}$) two-body quenching of XeF^* (low ν) measured in photolysis of XeF_2 . In terms of the mechanism above, we postulate that the $\text{KrXe}^* + \text{F}_2$ reaction does not produce XeF^* ; rather, the initially formed vibrationally excited KrXeF^* molecule subsequently dissociates, not to $\text{XeF}^* + \text{Kr}$, but to $\text{Kr} + \text{Xe} + \text{F}$ because of the ionic-covalent surface crossing for KrXeF^* . Thus, the apparent quenching of XeF^* in the $\text{Xe}/\text{F}_2 + \text{Kr}$ sensitization experiments is via Reactions (3) + (5), with the latter having $\text{Kr} + \text{Xe} + 2\text{F}$ as the exit channel. In the photolysis experiments the XeF^* (low ν) is quenched directly by a two-body collision.

As already discussed in the above paragraph, two-body quenching of XeF^* by Xe and Kr is expected because of the instability of the Xe_2F^* and KrXeF^* trimer molecules. This conclusion is consistent with our XeF^* quenching studies,^{12,26} but not necessarily with

all other views²⁵ of XeF* quenching by Xe or Kr. In contrast to XeF*, the quenching of XeCl* and KrF* by Kr and Ar, respectively, could be dominated by three-body quenching since KrXeCl* and ArKrF* have bound states. Quenching of KrF* by Ar does have a large three-body rate constant ($k = 1 \times 10^{-31} \text{ cm}^6 \text{ s}^{-1}$)^{27,28} in agreement with this argument. The quenching of XeCl* by Kr has not yet been studied in detail. By extension of these arguments, three-body quenching of KrX* by He and Ne and XeF* by He, Ne, and Ar should be slow, at least, via formation of the mixed rare gas trimers. The three-body quenching of KrF* by He and Ne is less than 10^{-33} and $10^{-32} \text{ cm}^6 \text{ s}^{-1}$, respectively.²⁸ The three-body quenching of XeF* by Ne is comparable²⁵ ($\sim 5 \times 10^{-33} \text{ cm}^6 \text{ s}^{-1}$); there is no consensus three-body rate constant for He but the quenching is slow.^{12,26,24} Early workers^{30,31} assigned quenching of XeF* by Ar to a three-body process with a rate constant of $2.7 \times 10^{-32} \text{ cm}^6 \text{ s}^{-1}$; but this interpretation of the slow quenching has been challenged.^{26,29} In conclusion, the three-body quenching data for XeF* and KrF* are, at least, in qualitative agreement with the present observations of the mixed rare gas halide trimers.

ACKNOWLEDGMENT

This work was supported by the U. S. Dept. of Energy (DE-AC02-80ET33068).

- ¹D. C. Lorents, D. L. Huestis, M. V. McCusker, H. H. Nakano, and R. M. Hill, *J. Chem. Phys.* **68**, 4657 (1978).
- ²C. H. Chen, M. G. Payne, and J. P. Judish, *J. Chem. Phys.* **69**, 1626 (1978).
- ³J. A. Mangano, J. H. Jacob, M. Rokni, and A. Hawryluk, *Appl. Phys. Lett.* **31**, 26 (1977).
- ⁴F. K. Tittel, W. L. Wilson, R. E. Stickel, G. Marowsky, and W. E. Ernst, *Appl. Phys. Lett.* **36**, 405 (1980).
- ⁵(a) W. R. Wadt and P. J. Hay, *J. Chem. Phys.* **68**, 3850 (1978); (b) W. R. Wadt and P. J. Hay, *Appl. Phys. Lett.* **30**, 573 (1977).
- ⁶D. L. Huestis and N. E. Schlotter, *J. Chem. Phys.* **69**, 3100 (1978).
- ⁷H. C. Brashears and D. W. Setser, *J. Phys. Chem.* **84**, 224 (1980).
- ⁸N. G. Basov, V. A. Nanylychev, V. A. Dolgikh, O. M. Kerimov, V. S. Lebedev, and A. G. Molchanov, *JETP Lett.* **26**, 17 (1977).
- ⁹T. Dreiling, H. C. Brashears, and D. W. Setser, *J. Chem. Phys.* (to be submitted).
- ¹⁰A. C. Vikis, *Chem. Phys. Lett.* **57**, 522 (1978).
- ¹¹E. H. Fink, D. Wallach, and C. B. Moore, *J. Chem. Phys.* **56**, 3608 (1972).
- ¹²H. C. Brashears and D. W. Setser, *Appl. Phys. Lett.* **33**, 821 (1978).
- ¹³T. Tellinghuisen and M. R. McKeever, *Chem. Phys. Lett.* **72**, 94 (1980).
- ¹⁴H. C. Brashears, Jr., D. W. Setser, and Y.-C. Yu, *J. Phys. Chem.* **84**, 2225 (1980).
- ¹⁵J. H. Kolts, J. E. Velazco, and D. W. Setser, *J. Chem. Phys.* **71**, 1247 (1979).
- ¹⁶J. H. Kolts and D. W. Setser, *J. Chem. Phys.* **68**, 4848 (1978).
- ¹⁷T. Oka, M. Kogoma, M. Imamura, and S. Arai, *J. Chem. Phys.* **70**, 3384 (1979).
- ¹⁸T. D. Bonifield, K. H. K. Rambow, G. K. Walters, M. V. McCusker, and D. C. Lorents, *J. Chem. Phys.* **72**, 2914 (1980).
- ¹⁹R. Thornton, E. D. Poliakoff, E. Matthias, S. H. Southworth, R. A. Rosenberg, W. G. White, and D. A. Shirley, *J. Chem. Phys.* **71**, 133 (1979).
- ²⁰(a) J. H. Kolts, J. E. Velazco, and D. W. Setser, *J. Chem. Phys.* **71**, 1247 (1979); (b) D. W. Setser, T. Dreiling, H. C. Brashears, Jr., and J. C. Kolts, *Faraday Discuss. Chem. Soc.* **67**, 255 (1979).
- ²¹C. Y. Ny, P. W. Tidemann, B. H. Mahan, and Y. T. Lee, *J. Chem. Phys.* **66**, 5737 (1977).
- ²²G. P. Quigley and W. M. Hughes, *Appl. Phys. Lett.* **32**, 649 (1978).
- ²³(a) J. H. Kolts, Ph.D. Thesis, Kansas State University, Manhattan, Kansas (1978); (b) M. P. Casassa, M. F. Golde, and A. Kvaran, *Chem. Phys. Lett.* **59**, 51 (1978).
- ²⁴J. G. Eden and R. W. Waynant, *J. Chem. Phys.* **68**, 2850 (1978).
- ²⁵D. W. Trainor, J. H. Jacob, and M. Rokni, *J. Chem. Phys.* **72**, 3646 (1980).
- ²⁶H. C. Brashears and D. W. Setser, *J. Phys. Chem.* (to be published).
- ²⁷M. Rokni, J. H. Jacob, and J. A. Mangano, *Phys. Rev. A* **16**, 2216 (1977).
- ²⁸J. G. Eden, R. W. Waynant, S. K. Searles, and R. Burnham, *J. Appl. Phys.* **49**, 5363 (1978).
- ²⁹G. Black, R. L. Sharpless, D. C. Lorents, R. Gutcheck, T. Bonifield, D. Helms, and G. K. Walters, presented at "Topical Meeting on Eximer Lasers," Charleston, South Carolina (1979).
- ³⁰M. Rokni, J. H. Jacob, J. A. Mangano, and R. Brochu, *Appl. Phys. Lett.* **30**, 458 (1977).
- ³¹J. G. Eden and R. W. Waynant, *Opt. Lett.* **2**, 13 (1978).